Cell Host & Microbe
Short Article

Host-Parasite Interactions Revealed by *Plasmodium falciparum* Metabolomics

Kellen L. Olszewski,[1,2] Joanne M. Morrisey,[4] Daniel Wilinski,[1,2] James M. Burns,[4] Akhil B. Vaidya,[4] Joshua D. Rabinowitz,[2,3] and Manuel Llinás[1,2,*]
[1]Department of Molecular Biology
[2]Lewis-Sigler Institute for Integrative Genomics
[3]Department of Chemistry
Princeton University, Princeton, NJ 08544, USA
[4]Center for Molecular Parasitology, Department of Microbiology and Immunology, Drexel University College of Medicine, Philadelphia, PA 19129, USA
*Correspondence: manuel@genomics.princeton.edu
DOI 10.1016/j.chom.2009.01.004

SUMMARY

Intracellular pathogens have devised mechanisms to exploit their host cells to ensure their survival and replication. The malaria parasite *Plasmodium falciparum* relies on an exchange of metabolites with the host for proliferation. Here we describe a mass spectrometry-based metabolomic analysis of the parasite throughout its 48 hr intraerythrocytic developmental cycle. Our results reveal a general modulation of metabolite levels by the parasite, with numerous metabolites varying in phase with the developmental cycle. Others differed from uninfected cells irrespective of the developmental stage. Among these was extracellular arginine, which was specifically converted to ornithine by the parasite. To identify the biochemical basis for this effect, we disrupted the plasmodium arginase gene in the rodent malaria model *P. berghei*. These parasites were viable but did not convert arginine to ornithine. Our results suggest that systemic arginine depletion by the parasite may be a factor in human malarial hypoargininemia associated with cerebral malaria pathogenesis.

INTRODUCTION

Infection by the malaria parasite *Plasmodium falciparum* has severe and potentially lethal consequences for the metabolic state of the human host (Planche et al., 2005). The approximately 500 million cases of this devastating disease lead each year to 1–2 million deaths worldwide (Sachs and Malaney, 2002). In all parasitic infections there is a significant metabolic interaction between pathogen and host as the parasite diverts nutrients toward its own growth while the host struggles to maintain homeostasis and cope with waste products, toxins, and tissue damage. In the case of *P. falciparum*-induced malaria, the metabolic demands of the rapidly proliferating parasite cells, coupled with the effects of massive erythrocyte lysis and ischemic damage arising from the sequestration of parasitized erythrocytes within the microvasculature, are responsible for the pathogenesis of the disease and its manifestations (Mackintosh et al., 2004). These clinical manifestations include hypoglycemia, lactic acidosis, hemolytic anemia, hemoglobinuria, and hypoargininemia.

The metabolites required by cells for macromolecular synthesis and growth are either acquired directly by uptake from the environment or else biosynthesized from the pool of available nutrients. Free-living protozoa maintain a versatile and dynamically regulated metabolic network that can support optimal growth from a wide variety of nutrient sources. In contrast, obligate intracellular parasites of mammals are restricted to a much more homeostatic and nutrient-rich environment and might be expected to have adapted to this specific milieu by altering the architecture of their metabolic network to maximize growth at the cost of flexibility. Within the human host, *P. falciparum* is found mostly within mature erythrocytes in the nutritionally complex environment of the bloodstream, and a wealth of evidence suggests that the metabolism of these blood-stage parasites has diverged significantly from well-studied model eukaryotes such as yeast.

Upon invading an erythrocyte, the parasite induces major modifications to the host cell to permit the directed exchange of metabolites (reviewed in Kirk et al., 2005). New permeability pathways are induced on the host cell surface to enhance the influx and efflux of specific compounds. The parasite also initiates a catabolic process whereby hemoglobin from the erythrocyte cytoplasm is ingested and proteolyzed into its constituent amino acids in an acidic vacuole (Krugliak et al., 2002). Extensive genomic and biochemical evidence indicates that many areas of parasite metabolism have been radically streamlined or modified. For example, *Plasmodia* have lost the ability to synthesize the purine ring de novo, rendering them auxotrophs dependent on the uptake of purine nucleotides and nucleobases from the host (Gardner et al., 2002). These parasites are also incapable of amino acid biosynthesis, relying instead on hemoglobin catabolism and uptake from the extracellular space (Gardner et al., 2002). Energy metabolism consists almost entirely of glucose fermentation by the parasite to lactate, calling into question the role of the parasite mitochondrion in energy generation (Sherman, 1998). The function of the apicoplast, a nonphotosynthetic plastid-like organelle, remains poorly elucidated, although it is known to play a role in fatty acid, heme, and isoprenoid biosynthesis (Ralph et al., 2004).

Due to the importance of plasmodial metabolism for malaria pathogenesis and as a target for most current and candidate

antimalarial pharmaceuticals, it is critical that we understand both the structure and dynamics of the parasite metabolic network. Indirect approaches to reconstructing this network, such as inference from genomic data or in vitro biochemistry, are at best incomplete and present significant obstacles in the case of highly diverged organisms. Metabolomic technologies (Kell, 2004; Want et al., 2005), however, are beginning to enable systems-level measurements of changes in metabolic activity in response to genetic (Fischer and Sauer, 2003) and nutrient (Brauer et al., 2006) perturbations, as well as drug treatments (Nicholson et al., 2002) and other viral infections (Munger et al., 2006).

One focus of recent metabolomic investigations has been the nature of host-parasite interactions. Parasite pathogens and their hosts are by definition metabolically intertwined, and the pathology of many parasitic diseases is linked to dysregulation of host metabolism. Several studies have examined the systemic effects of parasite infection in vivo by nuclear magnetic resonance analysis of host biofluids with the aim of elucidating metabolic modulation by the parasite and identifying reliable biomarkers to aid in the diagnosis of *Schistosoma* (Wang et al., 2004), *Trichinella* (Martin et al., 2006), and *Plasmodium* (Li et al., 2008) infection. These studies have uncovered a number of significant effects that likely would not have been found by classical biochemical methods. In particular, an analysis of urine and plasma from mice infected by *Plasmodium berghei* (Li et al., 2008) discovered evidence of a disturbance of the gut microbiota and high levels of the lysine catabolic product pipecolic acid in host urine, an effect that thus far appears to be specific to plasmodial infection. Directed metabolomic experiments in cell culture have also revealed critical aspects of parasite metabolism, such as an apparent partitioning of carbon metabolism in the protozoan *Trypanosoma brucei* into different regimes corresponding to the differing nutrient availabilities in the mammalian and insect host tissues (Coustou et al., 2008). Recently, NMR metabolomics has also been used to determine the intracellular concentrations of a range of metabolites in the *P. falciparum* trophozoite stage (Teng et al., 2008). Applying metabolomic approaches to study the dynamics of *P. falciparum*-infected erythrocyte metabolism promises to similarly unravel some of the more poorly understood aspects of parasite biology.

Understanding the plasticity of *Plasmodium* metabolism to physiologically relevant perturbations will ultimately have great clinical relevance in light of the possibility that parasites experience dramatically different metabolic states within the human host, and the fact that certain front-line drugs, such as artemisinin and its derivatives, act via an entirely unknown mechanism. We have taken the initial step toward this goal by conducting a metabolomic study of the complete intraerythrocytic developmental cycle (IDC) of the most virulent human malaria parasite, *Plasmodium falciparum*.

RESULTS

P. falciparum-Infected Red Blood Cell Metabolite Analysis

We have quantitatively measured the levels of known metabolites in synchronized cultures of *P. falciparum* (3D7 strain) over the course of its 48 hr blood-stage developmental cycle using a liquid chromatography-tandem mass spectrometry (LC-MS/MS) method that simultaneously assays for ~200 compounds of validated identity (Lu et al., 2006). We analyzed both parasite-infected and uninfected red blood cell (RBC) cultures at seven time points during development to determine the parasite-induced alterations to normal RBC metabolism. The RBCs (infected and uninfected) and the liquid culture medium were collected and analyzed separately in order to profile the parasite-induced changes to both the intra- and extracellular metabolite pools. Roughly 90 metabolites were detected with a signal sufficient to construct temporal profiles of their relative levels (Figures 1, S1, and S2 and Tables S1 and S2). These compounds span a wide range of metabolic pathways and include amino acids, nucleotides, biosynthetic precursors, and central carbon metabolism intermediates. For comparative purposes, we also measured global parasite mRNA levels in parallel by DNA microarray analysis for all time points (Figure S3 and Table S3).

Due to the highly periodic nature of gene expression observed during the IDC (Bozdech et al., 2003), we analyzed our metabolite profiles for periodic fluctuation to determine if metabolic requirements are also cyclical. Although many metabolite levels were either unchanged or else varied monotonically throughout the cycle, the subset shown in Figure 1A exhibited detectable periodicity. Most of these metabolites show peak abundance during the late trophozoite/early schizont stages, a period of the IDC associated with high levels of energy metabolism and macromolecular biosynthesis.

The *P. falciparum* metabolome reflects the radical metabolic simplification that has occurred over its evolution toward a parasitic lifestyle. For example, we find no evidence for de novo amino acid biosynthesis, consistent with extensive genomic (Gardner et al., 2002) and biochemical (Krugliak et al., 2002) evidence that the *Plasmodia* have essentially lost this capacity entirely in favor of amino acid scavenging and hemoglobin catabolism. The metabolites that are detected and that appear by this analysis to be cell-cycle-regulated, are indicative of the major metabolic processes that are known to be essential for growth. For example, dihydro-orotate and orotate, intermediates in the pyrimidine biosynthesis pathway, oscillate strongly in phase with the IDC (Figure 1A). As the parasite's sole source of pyrimidine bases, this pathway is essential for growth and in fact has been proposed to be the effective target of the antimalarial drug atovaquone (Painter et al., 2007). Inosine-5′-phosphate (IMP) follows a similarly periodic profile (Figure 1A). This metabolite is the product of an early step in the salvage pathway by which the *Plasmodia*, which are obligate purine auxotrophs, acquire purine bases (Downie et al., 2008). These metabolites reach their peak abundance coincident with a burst of nucleosides and nucleoside monophosphates occurring 32–40 hr postinvasion (Figure 1A), corresponding to the late trophozoite/early schizont transition, in which the parasite successively replicates its genome 16–32 times and nucleotide demand is at its highest.

Energetically, it is well established that the *Plasmodia* rely almost entirely on glycolysis and perform little or no oxidative phosphorylation (Lang-Unnasch and Murphy, 1998). While the parasites possess a mitochondrion, the mitochondrial genome is the smallest sequenced to date, their oxygen consumption is minimal, and there has been no clear evidence of a functional

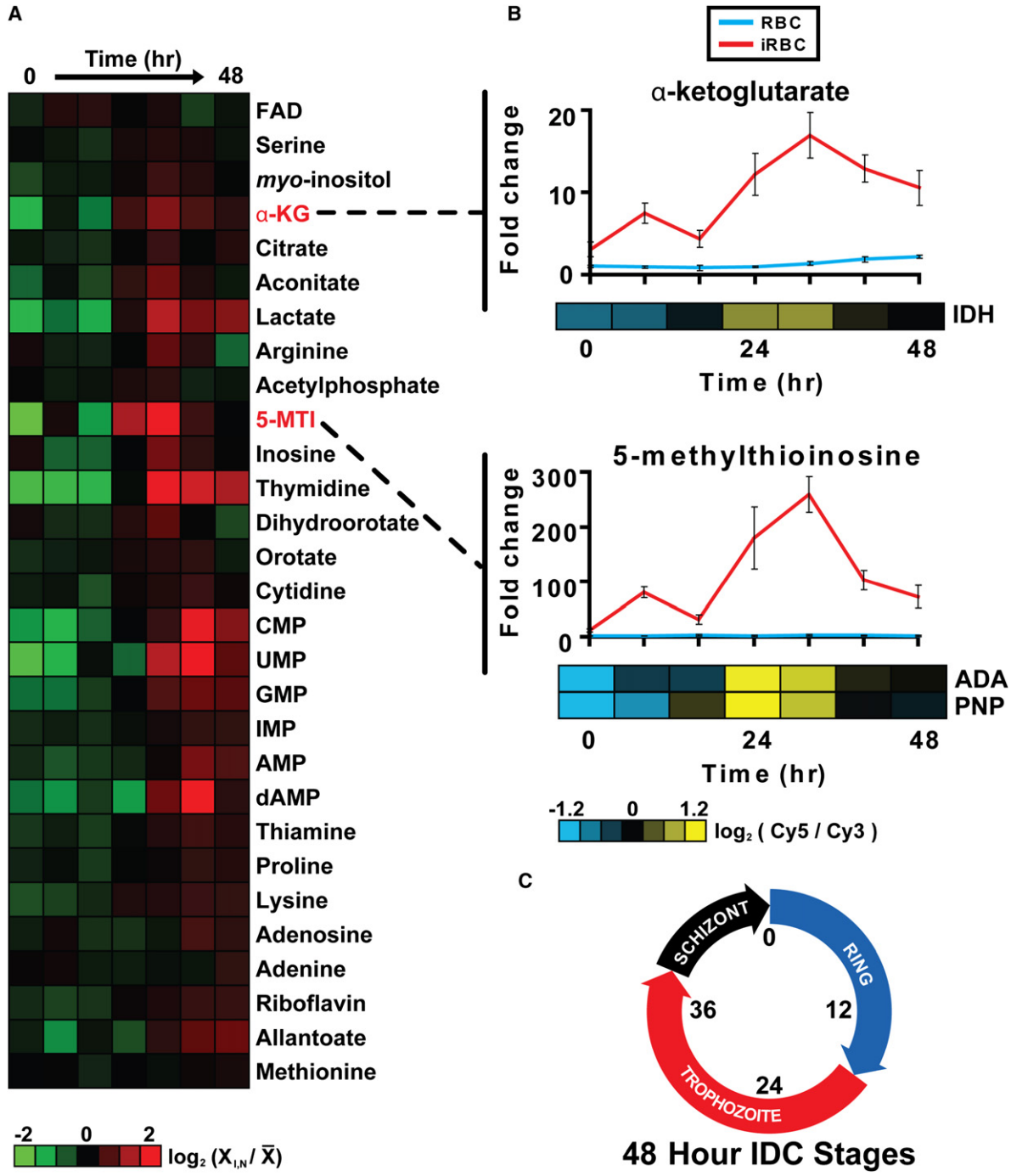

Figure 1. Periodic Metabolite Fluctuation during the Intraerythrocytic Developmental Cycle

(A) Profiles of 29 intracellular metabolites with periodic changes in relative levels. Relative levels are expressed as the mean-centered log ratio of the normalized signal intensity in the infected RBC extract at each time point ($X_{I,N}/\bar{X}$). Profiles are ordered by the timing of their peak abundance level, from early (top) to late (bottom).

(B) Temporal profile of relative levels of α-ketoglutarate and 5-methylthioinosine (5-MTI) levels in RBC (blue lines) and infected RBC (red lines) extracts over the IDC. Shown for comparison are the gene expression profiles of the associated enzymes isocitrate dehydrogenase (IDH), adenosine deaminase (ADA), and purine nucleoside phosphorylase (PNP) as determined by DNA microarray analysis. The error is given as the SD of n = 3 independent biological replicates.

(C) Schematic of the developmental stages during the 48 hr IDC.

tricarboxylic acid (TCA) cycle during the blood stages of growth (van Dooren et al., 2006). Strikingly, however, we observe coincident peaks in the TCA-cycle intermediates citrate, aconitate, and α-ketoglutarate during the trophozoite stage (Figure S4). Malate exhibited a periodicity score slightly below our significance threshold but is also most abundant during this stage. The *P. falciparum* genome encodes all the necessary enzymes to run a complete TCA cycle, and all are expressed during the IDC (Figure S4) (Bozdech et al., 2003); these data suggest that the enzymes are also active. In light of the recent observation that the sole pyruvate dehydrogenase encoded by the *P. falciparum* genome localizes to the apicoplast, where it presumably generates acetyl-CoA exclusively for fatty acid biosynthesis (Foth et al., 2005) instead of the TCA cycle, these data suggest TCA metabolism may be more complex and important than previously realized and is a promising candidate for future study.

Within the set of nonperiodic metabolites, we find a substantial increase in the NAD+ content of infected RBCs, consistent with previous literature (Zerez et al., 1990). These high NAD+ levels are supported in part by biosynthesis from the precursor nicotinamide, which is significantly depleted from the culture medium during the late trophozoite/schizont stage of the life cycle (Figure S5). Elevated NAD+ levels have been suggested to be necessary to support the increased glycolytic flux in infected RBCs (Zerez et al., 1990). This flux upregulation is evident in our data as an increase in the relative rates of glucose consumption and lactate generation (Figure S5). These results agree with genomic data that suggest that *P. falciparum* should be entirely dependent on exogenous nicotinamide or nicotinic acid for NAD+ biosynthesis (Gardner et al., 2002) and highlight either the uptake or synthesis pathway as a potential drug target.

Metabolite and mRNA Transcript Abundance during Development

To better understand the relationship between gene expression and metabolite levels, we calculated the correlations between each intracellular metabolite profile and the mRNA expression profile of the enzymes involved in its formation or degradation (Table S4). Only a subset of metabolite-enzyme pairs are significantly correlated or anticorrelated. The strongest correlation was observed between 5-methylthioinosine (5-MTI), an intermediate in a *Plasmodium*-specific purine recycling pathway (Ting et al., 2005), and the upstream enzyme adenosine deaminase, although 5-MTI also correlates well with its downstream enzyme purine nucleoside phosphorylase (Figure 1B). Interestingly, α-ketoglutarate falls into this set due to its high correlation with isocitrate dehydrogenase (Figure 1B). No significant correlation is found between α-ketoglutarate and glutamate dehydrogenase, despite the presumptive major role of this enzyme in α-ketoglutarate formation. This points to the possibility that, despite the possibly noncanonical nature of the plasmodium TCA cycle, intracellular α-ketoglutarate levels are strongly impacted by the activity of canonical TCA cycle enzymes.

Arginine Is Rapidly and Specifically Depleted from the Culture Medium

P. falciparum digests up to 75% of its host cell hemoglobin (Hb) over its IDC to supply amino acids for protein synthesis and clear space within the host cell (Krugliak et al., 2002). Although the parasite lacks any capacity for de novo amino acid biosynthesis (Gardner et al., 2002), this process generates sufficient amounts of most amino acids to sustain growth even in the absence of external supplementation (Liu et al., 2006). We find that intracellular levels of the amino acids that are most abundant in hemoglobin (alanine, valine, and histidine) all rise significantly in the trophozoite stage, coincident with the initiation of hemoglobin digestion (Figure S1). These amino acids also accumulate in the extracellular medium, consistent with the observation that the parasite incorporates only a fraction of the Hb-derived amino acids into protein, excreting the excess as waste (Figures 2A and S2).

The most dramatic relative change in extracellular amino acid levels occurs for the nonproteogenic amino acids ornithine and citrulline, which accumulate substantially in the medium during trophozoite and schizont stages (Figure 2A). These amino acids are generally derived from arginine, which is significantly depleted over the same time interval (Figure 2A). Standard RPMI 1640 medium used for *Plasmodium* culturing contains 1.15 mM arginine, which represents an 8- to 10-fold excess over normal human serum arginine levels (Lopansri et al., 2003). However, previous studies have concluded that arginine is unnecessary to support optimal parasite growth (Liu et al., 2006), which suggests that the parasite acquires sufficient quantities of arginine from hemoglobin digestion. This raises the question of the origin and nature of the observed effect on arginine and its downstream metabolites. Intriguingly, several clinical studies have demonstrated a strong correlation between reduced plasma arginine levels and advanced malaria in both child and adult malaria patients (Lopansri et al., 2003; Yeo et al., 2007).

Arginine Depletion Is Due to Arginase

When we measured arginine, ornithine, and citrulline levels in a time course initiated during the trophozoite stage, arginine levels were depleted to almost undetectable levels over 40 hr (>100-fold down) (Figure 2B). In eukaryotic systems, there are several enzymes that can interconvert between arginine, ornithine, and citrulline, including arginase, nitric oxide synthase (NOS), and ornithine transcarbamylase. To determine which of these might be responsible for the observed effect, we cultured parasites in RPMI 1640 supplemented with equimolar amounts of unlabeled and uniformly $^{13}C^{15}N$-labeled L-arginine. After 40 hr, the only labeled form of ornithine detected was the fully $^{13}C^{15}N$-labeled form (Figure 3A). Fully labeled ornithine can be generated from fully labeled arginine directly by arginase-catalyzed hydrolysis of arginine to ornithine and urea, or indirectly by the action of a citrullinase on fully labeled citrulline to yield ornithine and ammonia. There is no recognizable citrullinase in the *P. falciparum* genome, but an arginase (PFI0320w) has been cloned and characterized (Muller et al., 2005). We therefore identify this enzyme as the likely source of extracellular ornithine. We also detected fully labeled citrulline, which might derive from labeled arginine via the removal of the terminal nitrogen atom by either NOS (yielding nitric oxide) or arginine deiminase (yielding ammonia). Neither of these enzymes is predicted in the *P. falciparum* genome, but human RBCs contain NOS protein that has been shown to be active under some circumstances

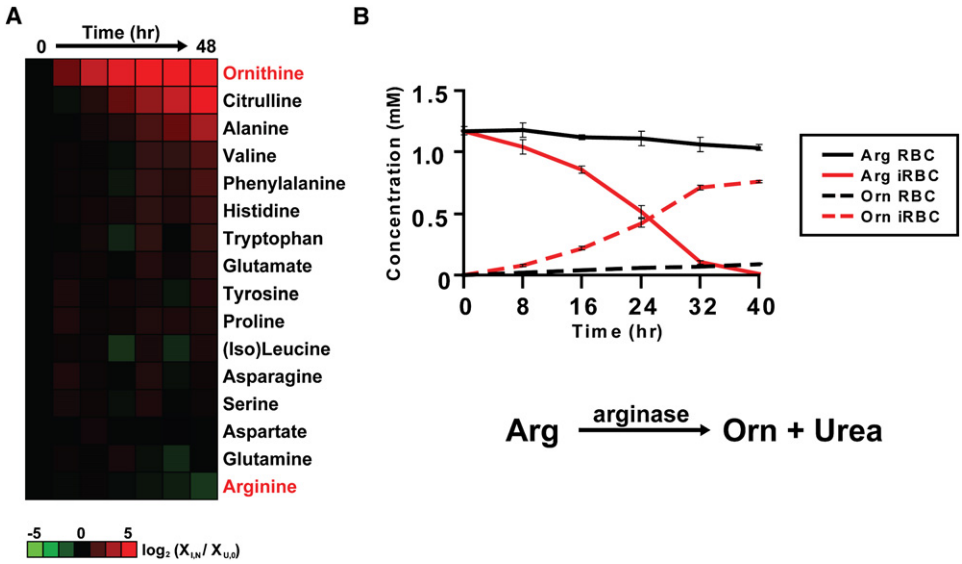

Figure 2. Amino Acid Levels in the Culture Medium

(A) Profiles of the 16 amino acids measured in culture medium samples. Relative levels are expressed as the background-subtracted log ratio of the normalized signal intensity in the infected RBC sample at each time point ($X_{I,N}$) to the normalized signal intensity in the uninfected RBC time 0 sample ($X_{U,0}$). Amino acids are ordered by the log ratio of the final time point, from highest (accumulating) (top) to lowest (depleting) (bottom).

(B) Arginine and ornithine concentrations in the culture medium of a 40 hr culture. A synchronized culture (6% initial parasitemia) was adjusted to 1% hematocrit in fresh RPMI 1640 culture medium at the trophozoite stage (approximately 24 hr postinfection) and incubated 40 hr in parallel with an uninfected RBC control culture. Concentrations were determined by LC-MS/MS analysis using an internal standard solution containing known concentrations of isotopically labeled arginine and ornithine. The error is given as the SD of n = 3 independent biological replicates.

(Kleinbongard et al., 2006). However, ornithine accounts for the majority of the depleted arginine (Figure 2B).

The *P. falciparum* Arginase Is Responsible for Arginine Turnover

The *P. falciparum* arginase I homolog (Muller et al., 2005) contains no recognizable targeting or export signal motifs and is most highly expressed during ring and schizont stages (Bozdech et al., 2003). However, mature human erythrocytes also contain active arginase I (NP_000036), and we observe arginine depletion and ornithine formation in uninfected blood cultures, although to a much lower degree (Figure 2B). One explanation for the enhanced arginase activity in parasite-infected cultures is the release of host arginase during RBC lysis, permitting continuous degradation of the extracellular arginine pool. This lysis-mediated effect has been proposed to explain the observed hypoargininemia in sickle-cell disease patients (Morris et al., 2005) due to the rupturing of sickled erythrocytes. To test the contribution of RBC lysis to in vitro arginine degradation, we incubated a culture consisting of uninfected RBCs that had been uniformly disrupted by hypotonic lysis in parallel with an infected RBC culture. The ornithine levels in the lysate culture were significantly lower than in the infected RBC culture, demonstrating that even 100% RBC lysis is insufficient to account for the high level of arginase activity (Figure 3B). This implicates the parasite arginase as the major factor in arginine depletion.

Arginase Knockout Parasites Exhibit Background Arginine Degradation Rates

To further test this hypothesis, we generated an arginase knockout (argKO) line of the mouse parasite *Plasmodium berghei* (ANKA strain) via site-specific recombination (Figure S6). The argKO line exhibited a slight delay in ascending parasitemia, but mice infected with WT and argKO consistently developed comparably high blood parasitemias (Figure S7) and exhibited no difference in the onset of morbidity, establishing that the parasite arginase is not essential for in vivo growth during the IDC. When cultured ex vivo, WT *P. berghei* exhibited high levels of ornithine generation, while ornithine generation by argKO parasites was indistinguishable from that of uninfected RBCs (Figure 4A). Energy metabolism, as measured by lactate excretion, was highly similar in WT and argKO parasites (Figure 4B); the slightly elevated lactate levels in the argKO 12 hr time point may reflect the added energetic demand of generating ornithine by an alternative pathway, such as proline degradation. Thus, high levels of arginase activity are found in a murine malaria parasite as well, but the enzyme does not significantly contribute to in vivo growth and thus may serve a secondary purpose.

DISCUSSION

Host-pathogen interactions rely heavily on an exchange of nutrients between the host cell and the infectious agent. Using a comprehensive mass spectrometry-based approach, we have demonstrated that development of *Plasmodium falciparum* within RBCs modulates the levels of dozens of compounds from most major metabolic processes, including amino acid and nucleotide metabolism, energy generation, and cellular redox potential. These data suggest a complex interplay between the host RBC and the parasite for nutrient acquisition, turnover, and waste removal.

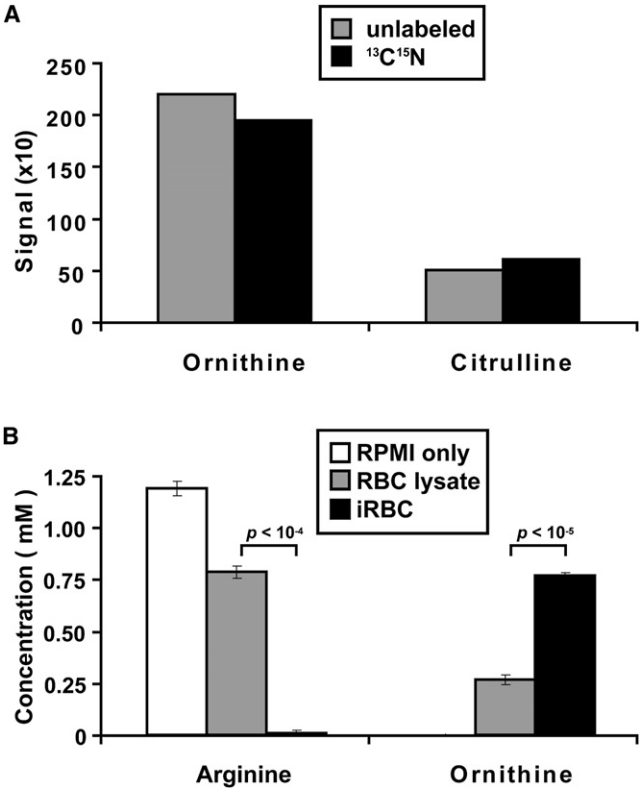

Figure 3. Arginine Depletion Is Due to the *P. falciparum* Arginase

(A) *P. falciparum* was cultured for 40 hr in RPMI 1640 medium supplemented with equimolar amounts (1.15 mM) of unlabeled and U-$^{13}C^{15}N$-labeled arginine. Culture medium samples were analyzed by LC-MS/MS for labeling in metabolites downstream of arginine. Shown are the signal intensities for unlabeled (gray) and U-$^{13}C^{15}N$-labeled (black) ornithine and citrulline. These were the only forms detected for either amino acid.

(B) Uninfected RBCs were uniformly lysed in distilled H_2O, diluted to 1% hematocrit in RPMI 1640, and incubated alongside a *P. falciparum* culture (1% hematocrit, 6% initial parasitemia, trophozoite stage). After 40 hr, medium samples were collected and analyzed by LC-MS/MS. Shown are concentrations of arginine and ornithine in untreated RPMI medium (white bars), RPMI medium mixed with the RBC lysate for 40 hr (gray bars), and the extracellular medium from an infected RBC (iRBC) culture grown for 40 hr in RPMI (black bars). The error is given as the SD of n = 3 independent biological replicates.

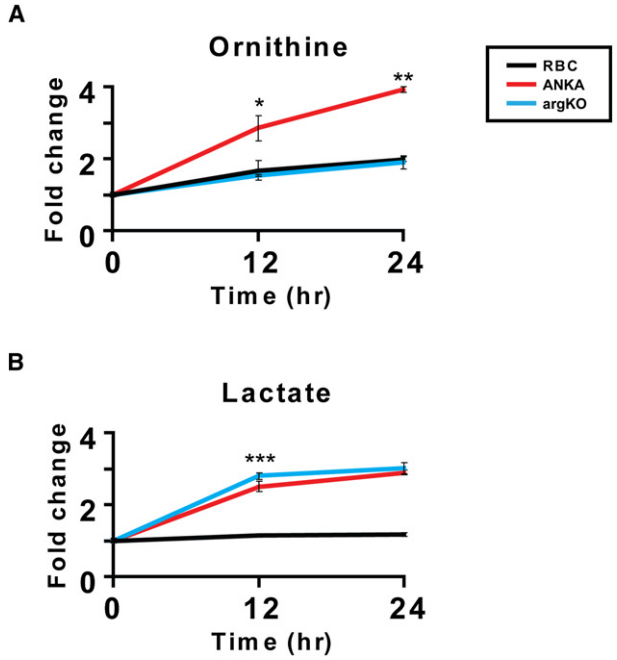

Figure 4. Phenotypic Analysis of the *P. berghei* Arginase Knockout Strain

(A) Ornithine levels in the culture medium of a 24 hr ex vivo culture (10% parasitemia, 1% hematocrit).

(B) Lactate levels from the same experiment. The *p* values give the significance of difference between the ANKA- and argKO-infected RBC samples (*$p < 0.01$; **$p < 10^{-4}$; ***$p < 0.05$). The error is given as the SD of n = 3 independent biological replicates.

Specifically, we have identified a rapid and specific degradation of arginine deriving from the plasmodial arginase. A major metabolic activity of arginases in protozoa is the generation of ornithine for polyamine biosynthesis (Kropf et al., 2005). However, this requirement seems unlikely to account for the high levels of observed activity for two reasons: first, the vast majority of the metabolized arginine is excreted into the extracellular environment, not selectively retained in the cell; second, the growth rate is not affected by the absence of arginine in the culture medium, suggesting that arginine is not rate-limiting for growth in vitro (Liu et al., 2006). The argKO parasites presumably acquire sufficient amounts of ornithine either from the plasma or the activity of the host cell arginase.

An alternative model is that the parasite depletes the host arginine pool in order to modulate the activity of the host enzyme, NOS. NOS is used by the mammalian immune system to generate antimicrobial nitric oxide (NO) radicals from arginine. Previous studies in rodent malaria models have found that, upon *Plasmodium* infection, the expression and activity of NOS is induced in activated macrophages (Tachado et al., 1996). Depletion of the plasma arginine pool may suppress this immune response by removing the substrate for NO production. In addition, the excess ornithine generated could exert a further suppressive effect by competing with arginine for transporter-mediated uptake into macrophages. A similar strategy is employed by the enterobacterium *Helicobacter pylori*, which uses its arginase to deplete the host arginine pool and ablate the NOS response (Gobert et al., 2001). However, while NO directly suppresses *H. pylori* infection by killing the bacteria, this does not seem to be the case with *Plasmodium*. Reactive nitrogen intermediates have been shown to have direct antiparasitic activity in vitro, but only at concentrations orders of magnitude above physiological levels (reviewed in Sobolewski et al., 2005). In addition, a study using NOS-deficient mouse lines established that host NO production does not affect the proliferation of asexual-stage parasites (Favre et al., 1999). However, NO does inactivate the more vulnerable sexual-stage gametocytes that are generated during the IDC and taken up by the mosquito host (Naotunne et al., 1993). This pathway may have evolved as a means for the more abundant and metabolically active asexual parasites to protect gametocytes from NO-mediated inactivation, increasing infectivity and allowing for more efficient propagation. The need to protect gametocytes from

NO may become more acute for *P. falciparum* because of the longer period (~14 days) necessary for their maturation, during which the parasite needs to remain sequestered from circulation. A further consequence of hypoargininemia and low host NO levels may be the upregulation of host endothelial cell surface receptors such as ICAM-1 (intracellular adhesion molecule 1), which increases the ability of the parasitized RBCs to cytoadhere to the vascular endothelium and thus avoid passage through the spleen and clearance (Sherman et al., 2003).

There is substantial evidence linking hypoargininemia to malarial infection and progression to cerebral malaria (Gramaglia et al., 2006; Lopansri et al., 2003; Yeo et al., 2007), but the origin of this effect has not been established to date. Previously proposed explanations included dietary deficiencies, defects in arginine transport or biosynthesis, and the activity of the free host arginase (Gramaglia et al., 2006; Lopansri et al., 2003). Additionally, arginine levels are strongly regulated during the host inflammatory response, and hypoargininemia is a hallmark of both pathogenic inflammations, such as bacterial sepsis, and those due to traumatic insult (Satriano, 2004). Our results, however, demonstrate that the *Plasmodium* arginase plays a significant role in arginine depletion (at least in vitro) and that disruption of the parasite enzyme ablates this effect without compromising in vivo viability. It has recently been reported that diminished NO bioavailability plays a critical role in the onset of experimental cerebral malaria (ECM), leading to mortality (Gramaglia et al., 2006). The same study also found that hypoargininemia correlated with disease progression. This, coupled with a similar result from a clinical study of human cerebral malaria (Lopansri et al., 2003), suggests that *Plasmodium* arginase could be an important factor in cerebral malaria pathogenesis, although the observation that plasma arginine levels in patients with severe malaria (which includes a substantial parasite burden in the blood) are not significantly different than in those with moderately severe malaria (Yeo et al., 2007) highlights the likely multifactorial nature of arginine regulation. Arginine supplementation has recently been shown to improve endothelial function and increase exhaled NO levels in clinical malaria patients (Yeo et al., 2007). Our results suggest that a combination therapy that incorporates a parasite arginase inhibitor may be a promising target for future investigation.

Metabolomic analysis promises to significantly deepen our understanding of *Plasmodium* biology and the malaria disease state. It will be useful in determining the metabolic differences between phenotypically divergent strains and in elucidating the mechanism of action for poorly characterized drugs, by mapping responses at the metabolic level that are undetectable by such methods as microarray analysis. The ability to generate concurrent metabolomic and transcriptomic profiles will allow investigation of the relationship between enzyme expression and metabolite level. A recent analysis of the transcriptional profiles of *P. falciparum* isolated from clinical malaria patients suggested that in vivo parasites may exist in distinct physiological regimes corresponding to stress or starvation states that have not been observed in ex vivo cultures (Daily et al., 2007). As metabolic enzymes represent a significant portion of the genes differentially regulated between these states, metabolomic investigations of patient samples might significantly advance our understanding of malarial pathogenesis within the human host. Furthermore, this experimental system will provide a powerful tool to further investigate clinically important biochemical pathways in greater detail and elucidate the metabolomic response to physiologically relevant perturbations such as nutrient limitation, heat shock, and drug exposures.

EXPERIMENTAL PROCEDURES

P. falciparum Culturing and Metabolite Extraction

P. falciparum cultures were maintained and synchronized by standard methods, with slight modifications outlined in the Supplemental Data. RBCs (infected or uninfected) were pelleted and immediately serially extracted, first with four volumes of 100% methanol at −75°C for 15 min, then twice with one volume 80:20 methanol:water at 4°C. For the second and third extractions, the mixture was sonicated 15 min on ice in a water bath sonicator. The culture medium supernatants from each extraction were pooled and centrifuged free of cell debris and protein. Supernatants were diluted in 4 volumes of 100% methanol at −75°C and centrifuged. Samples were analyzed within 24 hr of their generation.

LC-MS/MS Instrumentation

LC-MS/MS was performed using a Shimadzu LC-10A HPLC system and a Phenomenex Luna aminopropyl column (250 mm × 2 mm with a 5 μm particle size) coupled to a Thermo Electron Corporation Finnigan TSQ Quantum Ultra triple quadrupole mass spectrometer. The data presented are means ± SD for n = 3 biological replicates. Data extraction, treatment, periodicity, and microarray correlation analyses are described in the Supplemental Data.

DNA Microarray Analysis

For each time point, 0.5 ml of packed RBC (10% parasitemia) was pelleted by centrifugation, washed once in PBS, and flash-frozen in liquid nitrogen. Total RNA isolation and aminoallyl cDNA labeling were as previously described (Bozdech et al., 2003). A pool of 3D7 total RNA from all IDC stages was generated as the reference sample. Microarray data have been deposited at the NCBI Gene Expression Omnibus (GEO) under accession number GSE14524.

Parasite Infections

Donor BALB/c mice were injected with *P. berghei* ANKA WT or argKO stabilates. Parasitemia was monitored by examining blood films. Donor mice infected with argKO parasites were treated with 10 mg/kg pyrimethamine once parasites were detectable.

Generation of ArgKO *P. berghei*

To generate the pL0001.1 knockout vector, DNA fragments flanking the predicted *P. berghei* ortholog of *Pfi0320w* (*Pb000787.03.0*) were cloned into the vector pL0001 flanking the pyrimethamine selectable marker *Toxoplasma gondii* DHFR-TS. Linearized plasmid DNA was transfected and pyrimethamine-resistant parasites recovered from BALB/c mice. Locus disruption and clonality of the population was verified by Southern blotting (Figure S6).

Ex Vivo Short-Term Cultures of *P. berghei*

Blood from infected BALB/c mice with 20%–30% parasitemia was collected in HEPES-buffered saline containing 10 U/ml heparin. Cells were centrifuged and resuspended in RPMI 1640 medium containing 20% fetal calf serum and 0.5% Albumax. Parasitemia was adjusted to 10% by dilution with uninfected RBCs. Cultures were set up in triplicate at 1% hematocrit in 24-well plates and incubated in chambers gassed with 90% N_2, 5% O_2, and 5% CO_2. Samples were collected at 0, 12, and 24 hr for metabolomic analysis.

SUPPLEMENTAL DATA

Supplemental Data include Supplemental Experimental Methods, Supplemental References, seven figures, and five tables and can be found online at http://www.cell.com/cellhostandmicrobe/supplemental/S1931-3128(09)00031-6.

ACKNOWLEDGMENTS

We thank B. Bennett, E. De Silva, D. Gresham, Y. Kwon, M. Szpara, and I. Zhu for critical discussions and reading of the manuscript; V. Schramm for

5-MTI and 5-MTA purified standards; A. Waters for plasmid pL0001; and S. Bajad for assistance with initial experimental setup. M.L. is funded by the Burroughs Wellcome Fund and an NIH Director's New Innovators award (1DP2OD001315-01). J.D.R. is funded by a Beckman Young Investigators award and an NSF CAREER award. M.L and J.D.R. receive support from the Center for Quantitative Biology (P50 GM071508). J.M.B. and A.B.V. are funded by NIH/NIAID. K.O. is funded by an NSF Graduate Research Fellowship.

Received: November 10, 2008
Revised: December 19, 2008
Accepted: January 22, 2009
Published: February 18, 2009

REFERENCES

Bozdech, Z., Llinas, M., Pulliam, B.L., Wong, E.D., Zhu, J., and DeRisi, J.L. (2003). The transcriptome of the intraerythrocytic developmental cycle of Plasmodium falciparum. PLoS Biol. *1*, E5.

Brauer, M.J., Yuan, J., Bennett, B.D., Lu, W., Kimball, E., Botstein, D., and Rabinowitz, J.D. (2006). Conservation of the metabolomic response to starvation across two divergent microbes. Proc. Natl. Acad. Sci. USA *103*, 19302–19307.

Coustou, V., Biran, M., Breton, M., Guegan, F., Riviere, L., Plazolles, N., Nolan, D., Barrett, M.P., Franconi, J.M., and Bringaud, F. (2008). Glucose-induced remodeling of intermediary and energy metabolism in procyclic Trypanosoma brucei. J. Biol. Chem. *283*, 16342–16354.

Daily, J.P., Scanfeld, D., Pochet, N., Le Roch, K., Plouffe, D., Kamal, M., Sarr, O., Mboup, S., Ndir, O., Wypij, D., et al. (2007). Distinct physiological states of Plasmodium falciparum in malaria-infected patients. Nature *450*, 1091–1095.

Downie, M.J., Kirk, K., and Mamoun, C.B. (2008). Purine salvage pathways in the intraerythrocytic malaria parasite Plasmodium falciparum. Eukaryot. Cell *7*, 1231–1237.

Favre, N., Ryffel, B., and Rudin, W. (1999). Parasite killing in murine malaria does not require nitric oxide production. Parasitology *118*, 139–143.

Fischer, E., and Sauer, U. (2003). Metabolic flux profiling of Escherichia coli mutants in central carbon metabolism using GC-MS. Eur. J. Biochem. *270*, 880–891.

Foth, B.J., Stimmler, L.M., Handman, E., Crabb, B.S., Hodder, A.N., and McFadden, G.I. (2005). The malaria parasite Plasmodium falciparum has only one pyruvate dehydrogenase complex, which is located in the apicoplast. Mol. Microbiol. *55*, 39–53.

Gardner, M.J., Hall, N., Fung, E., White, O., Berriman, M., Hyman, R.W., Carlton, J.M., Pain, A., Nelson, K.E., Bowman, S., et al. (2002). Genome sequence of the human malaria parasite Plasmodium falciparum. Nature *419*, 498–511.

Gobert, A.P., McGee, D.J., Akhtar, M., Mendz, G.L., Newton, J.C., Cheng, Y., Mobley, H.L., and Wilson, K.T. (2001). Helicobacter pylori arginase inhibits nitric oxide production by eukaryotic cells: a strategy for bacterial survival. Proc. Natl. Acad. Sci. USA *98*, 13844–13849.

Gramaglia, I., Sobolewski, P., Meays, D., Contreras, R., Nolan, J.P., Frangos, J.A., Intaglietta, M., and van der Heyde, H.C. (2006). Low nitric oxide bioavailability contributes to the genesis of experimental cerebral malaria. Nat. Med. *12*, 1417–1422.

Kell, D.B. (2004). Metabolomics and systems biology: making sense of the soup. Curr. Opin. Microbiol. *7*, 296–307.

Kirk, K., Martin, R.E., Broer, S., Howitt, S.M., and Saliba, K.J. (2005). Plasmodium permeomics: membrane transport proteins in the malaria parasite. Curr. Top. Microbiol. Immunol. *295*, 325–356.

Kleinbongard, P., Schulz, R., Rassaf, T., Lauer, T., Dejam, A., Jax, T., Kumara, I., Gharini, P., Kabanova, S., Ozuyaman, B., et al. (2006). Red blood cells express a functional endothelial nitric oxide synthase. Blood *107*, 2943–2951.

Kropf, P., Fuentes, J.M., Fahnrich, E., Arpa, L., Herath, S., Weber, V., Soler, G., Celada, A., Modolell, M., and Muller, I. (2005). Arginase and polyamine synthesis are key factors in the regulation of experimental leishmaniasis in vivo. FASEB J. *19*, 1000–1002.

Krugliak, M., Zhang, J., and Ginsburg, H. (2002). Intraerythrocytic Plasmodium falciparum utilizes only a fraction of the amino acids derived from the digestion of host cell cytosol for the biosynthesis of its proteins. Mol. Biochem. Parasitol. *119*, 249–256.

Lang-Unnasch, N., and Murphy, A.D. (1998). Metabolic changes of the malaria parasite during the transition from the human to the mosquito host. Annu. Rev. Microbiol. *52*, 561–590.

Li, J.V., Wang, Y., Saric, J., Nicholson, J.K., Dirnhofer, S., Singer, B.H., Tanner, M., Wittlin, S., Holmes, E., and Utzinger, J. (2008). Global metabolic responses of NMRI mice to an experimental Plasmodium berghei infection. J. Proteome Res. *7*, 3948–3956.

Liu, J., Istvan, E.S., Gluzman, I.Y., Gross, J., and Goldberg, D.E. (2006). Plasmodium falciparum ensures its amino acid supply with multiple acquisition pathways and redundant proteolytic enzyme systems. Proc. Natl. Acad. Sci. USA *103*, 8840–8845.

Lopansri, B.K., Anstey, N.M., Weinberg, J.B., Stoddard, G.J., Hobbs, M.R., Levesque, M.C., Mwaikambo, E.D., and Granger, D.L. (2003). Low plasma arginine concentrations in children with cerebral malaria and decreased nitric oxide production. Lancet *361*, 676–678.

Lu, W., Kimball, E., and Rabinowitz, J.D. (2006). A high-performance liquid chromatography-tandem mass spectrometry method for quantitation of nitrogen-containing intracellular metabolites. J. Am. Soc. Mass Spectrom. *17*, 37–50.

Mackintosh, C.L., Beeson, J.G., and Marsh, K. (2004). Clinical features and pathogenesis of severe malaria. Trends Parasitol. *20*, 597–603.

Martin, F.P., Verdu, E.F., Wang, Y., Dumas, M.E., Yap, I.K., Cloarec, O., Bergonzelli, G.E., Corthesy-Theulaz, I., Kochhar, S., Holmes, E., et al. (2006). Transgenomic metabolic interactions in a mouse disease model: interactions of Trichinella spiralis infection with dietary Lactobacillus paracasei supplementation. J. Proteome Res. *5*, 2185–2193.

Morris, C.R., Kato, G.J., Poljakovic, M., Wang, X., Blackwelder, W.C., Sachdev, V., Hazen, S.L., Vichinsky, E.P., Morris, S.M., Jr., and Gladwin, M.T. (2005). Dysregulated arginine metabolism, hemolysis-associated pulmonary hypertension, and mortality in sickle cell disease. JAMA *294*, 81–90.

Muller, I.B., Walter, R.D., and Wrenger, C. (2005). Structural metal dependency of the arginase from the human malaria parasite Plasmodium falciparum. Biol. Chem. *386*, 117–126.

Munger, J., Bajad, S.U., Coller, H.A., Shenk, T., and Rabinowitz, J.D. (2006). Dynamics of the cellular metabolome during human cytomegalovirus infection. PLoS Pathog. *2*, e132.

Naotunne, T.S., Karunaweera, N.D., Mendis, K.N., and Carter, R. (1993). Cytokine-mediated inactivation of malarial gametocytes is dependent on the presence of white blood cells and involves reactive nitrogen intermediates. Immunology *78*, 555–562.

Nicholson, J.K., Connelly, J., Lindon, J.C., and Holmes, E. (2002). Metabonomics: a platform for studying drug toxicity and gene function. Nat. Rev. Drug Discov. *1*, 153–161.

Painter, H.J., Morrisey, J.M., Mather, M.W., and Vaidya, A.B. (2007). Specific role of mitochondrial electron transport in blood-stage Plasmodium falciparum. Nature *446*, 88–91.

Planche, T., Dzeing, A., Ngou-Milama, E., Kombila, M., and Stacpoole, P.W. (2005). Metabolic complications of severe malaria. Curr. Top. Microbiol. Immunol. *295*, 105–136.

Ralph, S.A., van Dooren, G.G., Waller, R.F., Crawford, M.J., Fraunholz, M.J., Foth, B.J., Tonkin, C.J., Roos, D.S., and McFadden, G.I. (2004). Tropical infectious diseases: metabolic maps and functions of the Plasmodium falciparum apicoplast. Nat. Rev. Microbiol. *2*, 203–216.

Sachs, J., and Malaney, P. (2002). The economic and social burden of malaria. Nature *415*, 680–685.

Satriano, J. (2004). Arginine pathways and the inflammatory response: interregulation of nitric oxide and polyamines: review article. Amino Acids *26*, 321–329.

Sherman, I.W. (1998). Carbohydrate Metabolism of Asexual Stages. In Malaria, Parasite Biology, Pathogenesis and Protection, I.W. Sherman, ed. (Washington, D.C.: ASM Press), pp. 135–143.

Sherman, I.W., Eda, S., and Winograd, E. (2003). Cytoadherence and sequestration in Plasmodium falciparum: defining the ties that bind. Microbes Infect. *5*, 897–909.

Sobolewski, P., Gramaglia, I., Frangos, J., Intaglietta, M., and van der Heyde, H.C. (2005). Nitric oxide bioavailability in malaria. Trends Parasitol. *21*, 415–422.

Tachado, S.D., Gerold, P., McConville, M.J., Baldwin, T., Quilici, D., Schwarz, R.T., and Schofield, L. (1996). Glycosylphosphatidylinositol toxin of Plasmodium induces nitric oxide synthase expression in macrophages and vascular endothelial cells by a protein tyrosine kinase-dependent and protein kinase C-dependent signaling pathway. J. Immunol. *156*, 1897–1907.

Teng, R., Junankar, P.R., Bubb, W.A., Rae, C., Mercier, P., and Kirk, K. (2008). Metabolite profiling of the intraerythrocytic malaria parasite *Plasmodium falciparum* by (1)H NMR spectroscopy. NMR Biomed., in press. Published online November 19, 2008. 10.1002/nbm.1323.

Ting, L.M., Shi, W., Lewandowicz, A., Singh, V., Mwakingwe, A., Birck, M.R., Ringia, E.A., Bench, G., Madrid, D.C., Tyler, P.C., et al. (2005). Targeting a novel Plasmodium falciparum purine recycling pathway with specific immucillins. J. Biol. Chem. *280*, 9547–9554.

van Dooren, G.G., Stimmler, L.M., and McFadden, G.I. (2006). Metabolic maps and functions of the Plasmodium mitochondrion. FEMS Microbiol. Rev. *30*, 596–630.

Wang, Y., Holmes, E., Nicholson, J.K., Cloarec, O., Chollet, J., Tanner, M., Singer, B.H., and Utzinger, J. (2004). Metabonomic investigations in mice infected with Schistosoma mansoni: an approach for biomarker identification. Proc. Natl. Acad. Sci. USA *101*, 12676–12681.

Want, E.J., Cravatt, B.F., and Siuzdak, G. (2005). The expanding role of mass spectrometry in metabolite profiling and characterization. ChemBioChem *6*, 1941–1951.

Yeo, T.W., Lampah, D.A., Gitawati, R., Tjitra, E., Kenangalem, E., McNeil, Y.R., Darcy, C.J., Granger, D.L., Weinberg, J.B., Lopansri, B.K., et al. (2007). Impaired nitric oxide bioavailability and L-arginine reversible endothelial dysfunction in adults with falciparum malaria. J. Exp. Med. *204*, 2693–2704.

Zerez, C.R., Roth, E.F., Jr., Schulman, S., and Tanaka, K.R. (1990). Increased nicotinamide adenine dinucleotide content and synthesis in Plasmodium falciparum-infected human erythrocytes. Blood *75*, 1705–1710.

Supplemental Data
Cell Host & Microbe, *Volume 5*

Host-Parasite Interactions Revealed by *Plasmodium falciparum* Metabolomics

Kellen L. Olszewski, Joanne M. Morrisey, Daniel Wilinski, James M. Burns, Akhil B. Vaidya, Joshua D. Rabinowitz, and Manuel Llinás

Supplemental Experimental Methods

P. falciparum Culturing

P. falciparum cultures were maintained and synchronized by standard methods (Lambros and Vanderberg, 1979; Trager and Jensen, 1976). Briefly, *P. falciparum* (3D7 strain) was maintained in RPMI 1640 culture medium supplemented with sodium bicarbonate (2 mg/mL), hypoxanthine (100 μM), Albumax II (0.25%) and gentamycin (50 μg/mL) in a humidified incubator at 5% CO_2, 6% O_2, and 37°C.

Forty-eight hour metabolite assays were carried out at either 0.5% (cell extract assay) or 1% (medium assay) hematocrit. A highly synchronized *P. falciparum* culture (10% parasitemia) was given fresh, prewarmed (37°C) media approximately 1 hour prior to the first timepoint, then split into 21 different flasks which served as N = 3 biological replicates per timepoint. For each assay, an uninfected RBC culture at the same hematocrit was started 24 hr prior to the experiment and then treated identically to the *P. falciparum* culture. At each timepoint of the intracellular metabolite timecourse, half the infected RBC sample was prepared for metabolite analysis and half was frozen in liquid nitrogen for microarray analysis.

LC-MS/MS Instrumentation

Liquid chromatography – tandem mass spectrometry (LC-MS/MS) was performed using an LC-10A HPLC system (Shimadzu, http://www.shimadzu.com) and a Luna aminopropyl column (250 mm × 2 mm with a 5-μm particle size from Phenomenex,

http://www.phenomenex.com) coupled to the mass spectrometer. The LC parameters were as follows: autosampler temperature, 4°C; injection volume, 20 μL; column temperature, 15°C; and flow rate, 150 μL/min. The LC solvents were Solvent A: 20 mM ammonium acetate + 20 mM ammonium hydroxide in 95:5 water:acetonitrile (pH 9.45); and Solvent B: acetonitrile. The gradients are as follows: positive mode, t = 0, 85% B; t = 15 min, 0% B; t = 28 min, 0% B; t = 30 min, 85% B; t = 40 min, 85% B; and negative mode, t = 0, 85% B; t = 15 min, 0% B; t = 38 min, 0% B; t = 40 min, 85% B; t = 50 min, 85% B.

Mass spectrometric analyses were performed on a Finnigan TSQ Quantum Ultra triple-quadrupole mass spectrometer (Thermo Electron Corporation, http://www.thermo.com), equipped with an electrospray ionization (ESI) source. ESI spray voltage was 3,200 V in positive mode and 3,000 V in negative mode. Nitrogen was used as sheath gas at 30 psi and as the auxiliary gas at 10 psi, and argon as the collision gas at 1.5 mTorr, with the capillary temperature 325°C. Scan time for each single reaction monitoring (SRM) event transition was 0.1 s with a scan width of 1 m/z. The LC runs were divided into time segments, with the SRM scans within each time segment limited to those compounds eluting during that time interval. For compounds eluting at the boundaries between time segments, the SRM scan corresponding to the compound is conducted in both time segments. The instrument control, data acquisition, and data analysis were performed by the Xcalibar software (Thermo Electron Corporation, version 1.4 SR1), which also controlled the chromatography system.

Data Treatment and Analysis

Metabolite levels were quantified by integrating peaks for each of the 188 SRMs using previously determined chromatographic retention times (Bajad et al., 2006; Lu et al., 2006) (additional new SRMs are listed in Table S5). The signal for each metabolite was defined as the height of the integrated peak. Metabolites were excluded from analysis if they failed to give a

signal greater than 1000 counts in any sample analyzed. Signals less than 100 counts were set to 100 (the approximate limit of detection) for the purposes of the analysis. Each metabolite signal was normalized to the signal of the internal standard U-^{13}C-succinate (negative mode) or U-^{13}C-UMP (positive mode) in the same sample to control for variation between runs. These normalized levels were averaged over the N = 3 replicates at each timepoint. All data are expressed as the ratio of the normalized levels of a metabolite in the sample at timepoint N ($X_{U/I,N}$) to the normalized levels of the same metabolite in the uninfected time 0 sample ($X_{U,0}$), to give the fold change in metabolite level relative to a fresh, uninfected RBC culture. For making heat maps, these ratios were $\log_2$-transformed and mean-centered (periodic data only), and visualized using Java Treeview (Saldanha, 2004). For statistical comparisons between samples, a two-tailed t test was employed.

For the periodicity analysis, the temporal profiles for each metabolite in infected RBC cell extracts were loaded into MATLAB® and the Curve Fitting Tool (*cftool()*) was used to find the sine curve (period = 48 hours) of the form:

$$y = a\sin((2\pi x)/48) + b) + c$$

that best fit the data. The R^2 value of the fit was used as a periodicity score, with profiles above the threshold $R^2 = 0.5$ defined as periodic. Metabolites were removed from this set if the correlation coefficient between their profiles in the infected and uninfected cultures was greater than 0.5 so as to disregard cases where the apparent periodicity was not a consequence of *P. falciparum* infection.

For the enzyme expression-metabolite level correlation analysis, a list of enzyme-metabolite pairs was manually curated from the "Malaria Parasite Metabolic Pathways" database (Ginsburg, 2006). For every intracellular metabolite measured, every metabolic enzyme that could directly produce or consume it was noted. Those enzymes for which we had gene expression data

from our DNA microarray analysis were compared to their paired metabolite by calculating the Pearson correlation coefficient between the log-transformed profiles of metabolite abundance and gene expression. These correlation values were scored for significance by permuting shuffling the metabolite-enzyme pairs 10,000 times, calculating the correlation coefficients between these shuffled pairs, and setting the coefficient at the 95^{th} percentile as the significance threshold.

DNA Microarray Analysis

For each timepoint, 0.5 mL of packed RBC (10% parasitemia) was pelleted by centrifugation, washed once in PBS and flash-frozen in liquid nitrogen. Total RNA isolation and amino-allyl cDNA labeling were as previously described (Bozdech et al., 2003). A pool of 3D7 total RNA from all intraerythrocytic developmental stages was generated and used as the reference sample. For DNA microarray hybridization, pool cDNA was coupled to Cy3 dye, while cDNA from an individual timepoint was coupled to Cy5 dye. DNA microarrays were scanned using an Axon 4200A scanner and images analyzed using Axon GenePix software (Axon Instruments, Union City, CA, USA). Microarray data were stored and analyzed using our in-house database PUMAdb (Princeton University MicroArray database). All data for individual arrays were normalized by a global normalization using unflagged features with ≥ 65% of pixels one or more standard deviations over local background. All unflagged spots were selected and extracted for further analysis. Data were filtered to remove oligos more than 1 datapoint missing across the timeseries, $\log_2$ transformed, mean centered, ordered by the timing of their peak expression level, and visualized with Java Treeview (Saldanha, 2004) (Table S3).

Generation of argKO *P. berghei*

To generate the pL0001.1 knockout vector, DNA fragments flanking the predicted *P. berghei* ortholog of *Pfi0320w* (*Pb000787.03.0*) were cloned into the vector pL0001 flanking the pyrimethamine selectable marker *Toxoplasma gondii* DHFR-TS. The 5' flanking region consisted

of a 848 bp fragment starting 742 bp upstream of the ATG start and extending 106 bp into the coding region [forward primer (*Apa*I): 5'-CCTTGG GGGCCC AAAGCAAAACAAGCAACCAAA-3'; reverse primer (*Hind*III): 5'- GGTTCC AAGCTT GCTAAGGGATTGACCAGCAG]; the 3' flanking region consisted of a 574 bp fragment starting 31 bp upstream of the stop codon and extending 543 bp downstream [forward primer (*Xba*I):CCTTGG TCTAGA TGCCAGAGTTCTAGGCAATG; reverse primer (*Sac*II):GGTTCC CCGCGG TGTGATCCGCATAAAAACCA]. The identities of both fragments were verified by sequencing.

The pL0001.1 plasmid was linearized by digestion with ApaI and SacII. Transfection of the plasmid and selection of knockout parasites generated through double a crossover event was carried out using the detailed protocol of Janse *et al* (Janse et al., 2006). Genomic DNA was isolated by standard methods from transfected parasites, digested with diagnostic restriction enzymes EcoRI and SpeI, subjected to electrophoresis and Southern blotting. The blots were probed with the 5' untranslated region of *P. berghei* arginase gene.

Growth Rate

Donor BALB/c mice were injected with *P. berghei* ANKA WT or argKO stabilates. Parasitemia was monitored by examining blood films. Mice infected with argKO parasites were treated with 10 mg/kg pyrimethamine once parasites were detectable. Blood from the donor mice was diluted and experimental mice in groups of 5 were inoculated with 10^6 parasites each. Parasitemia was monitored from day 3 after infection.

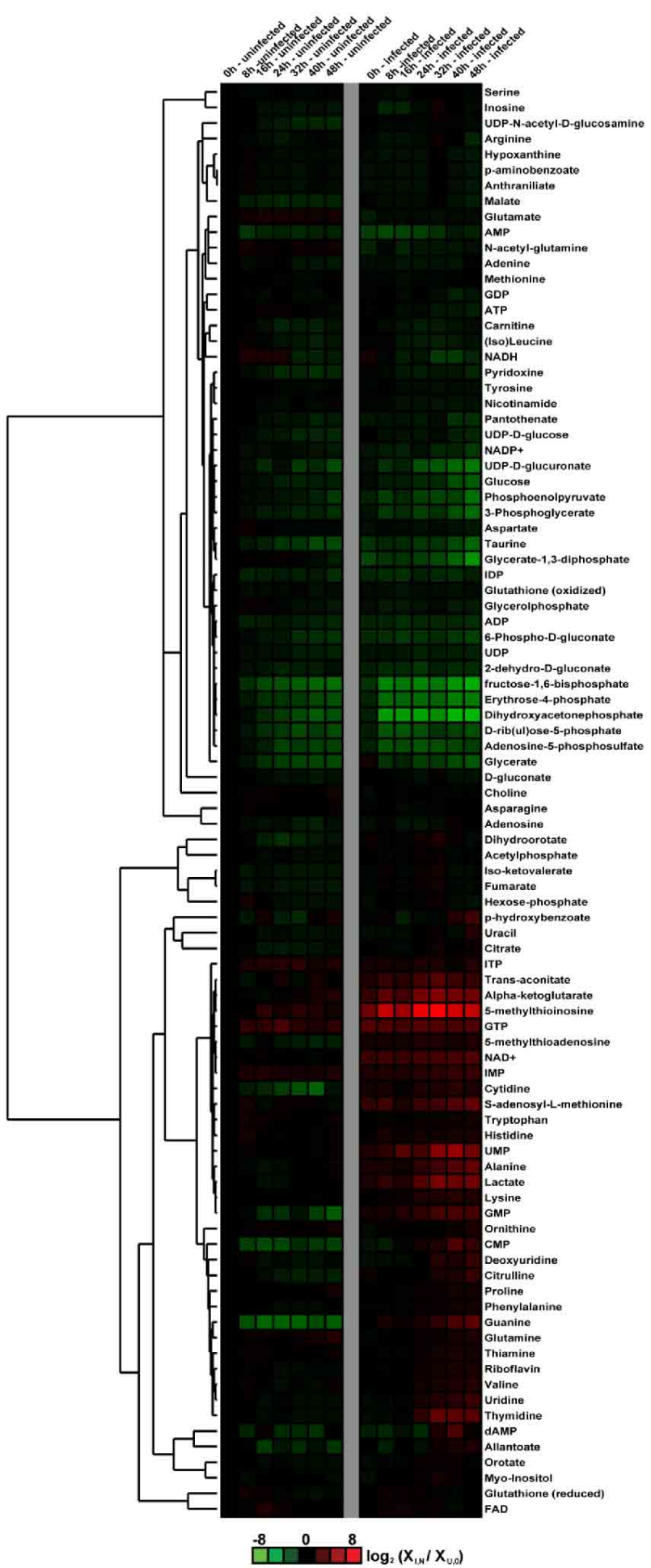

Figure S1. Clustering of Intracellular Metabolite Levels over the Intraerythrocytic Developmental Cycle

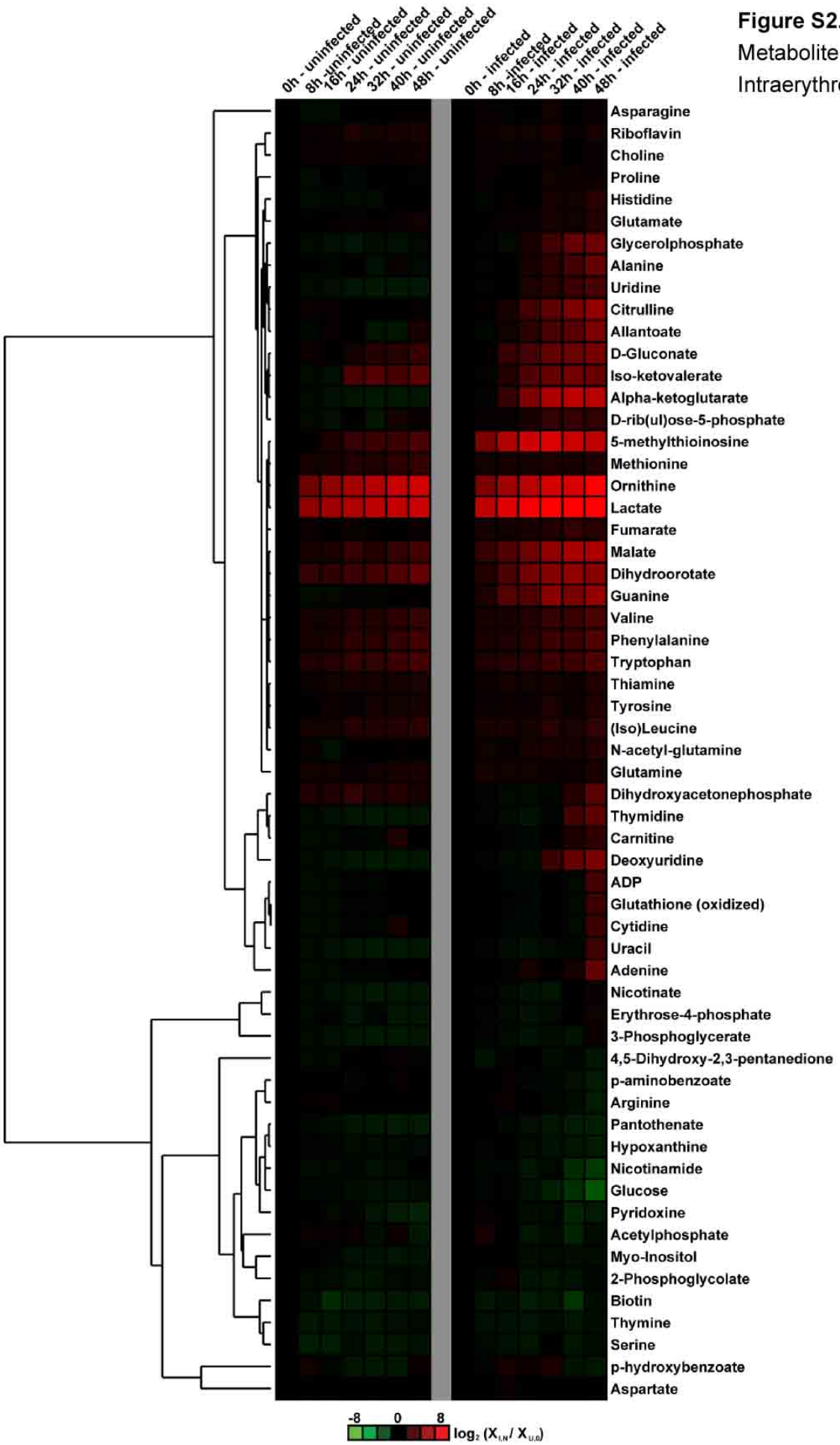

Figure S2. Clustering of Extracellular Metabolite Levels over the Intraerythrocytic Developmental Cycle

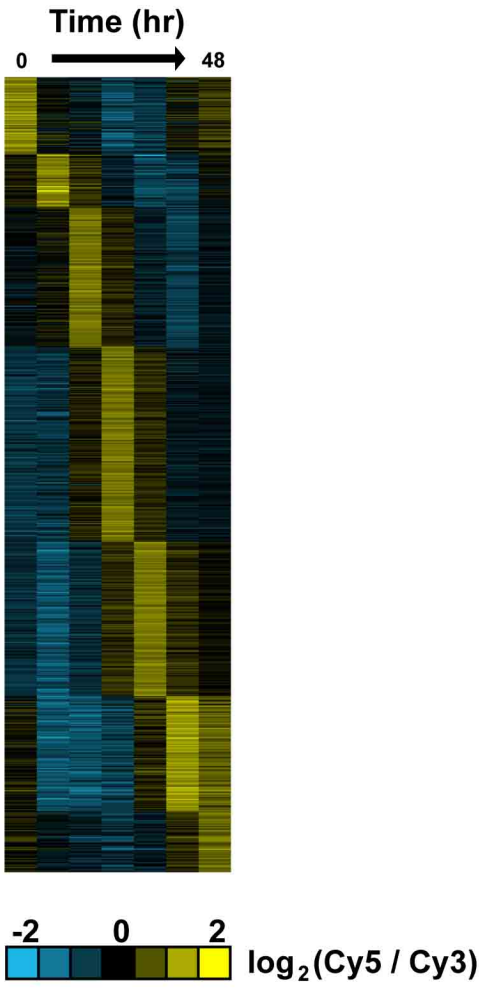

Figure S3. Gene Expression during the Intraerythrocytic Developmental Cycle

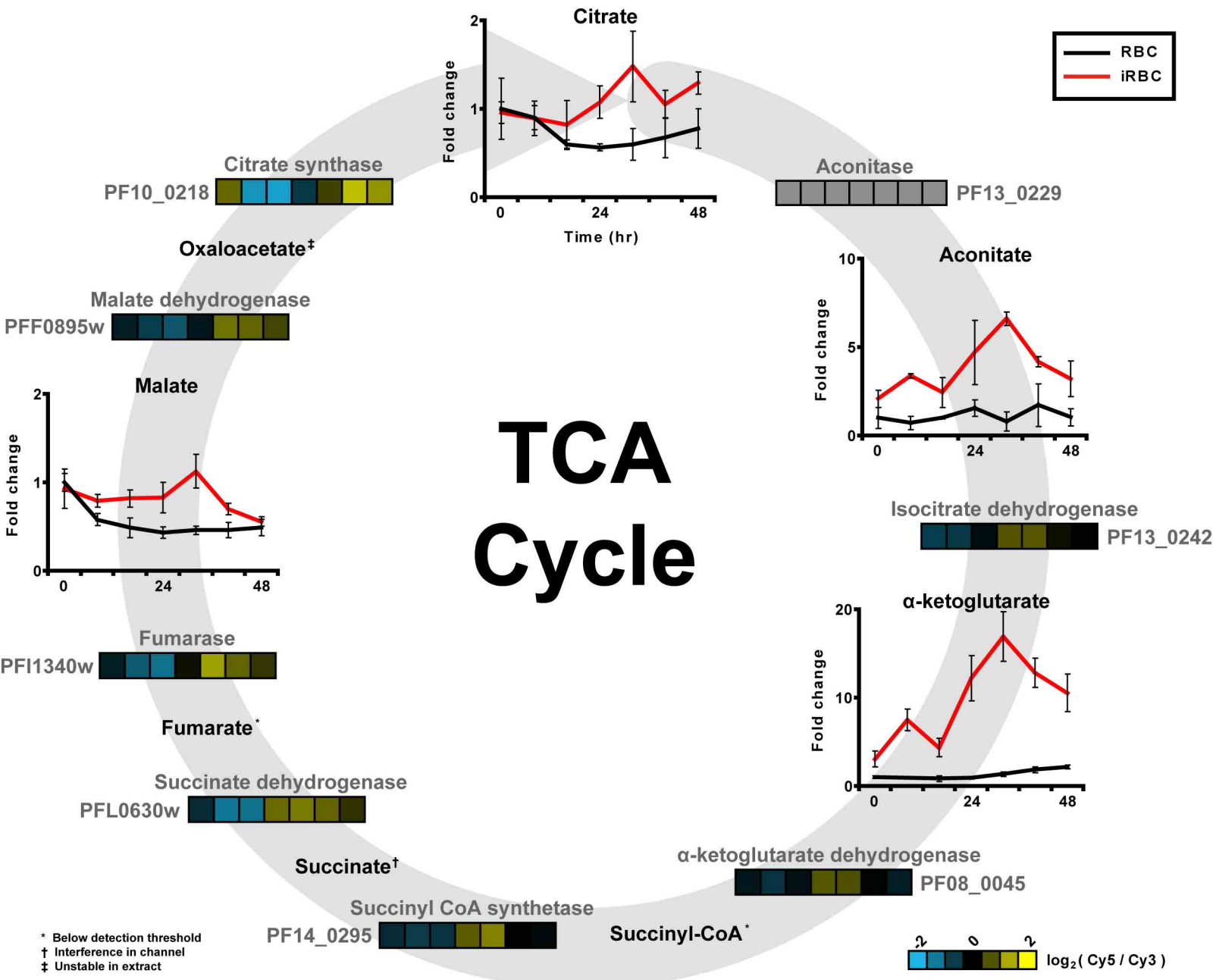

Figure S4. Tricarboxylic Acid Cycle Intermediates and Enzyme Levels Vary over the IDC

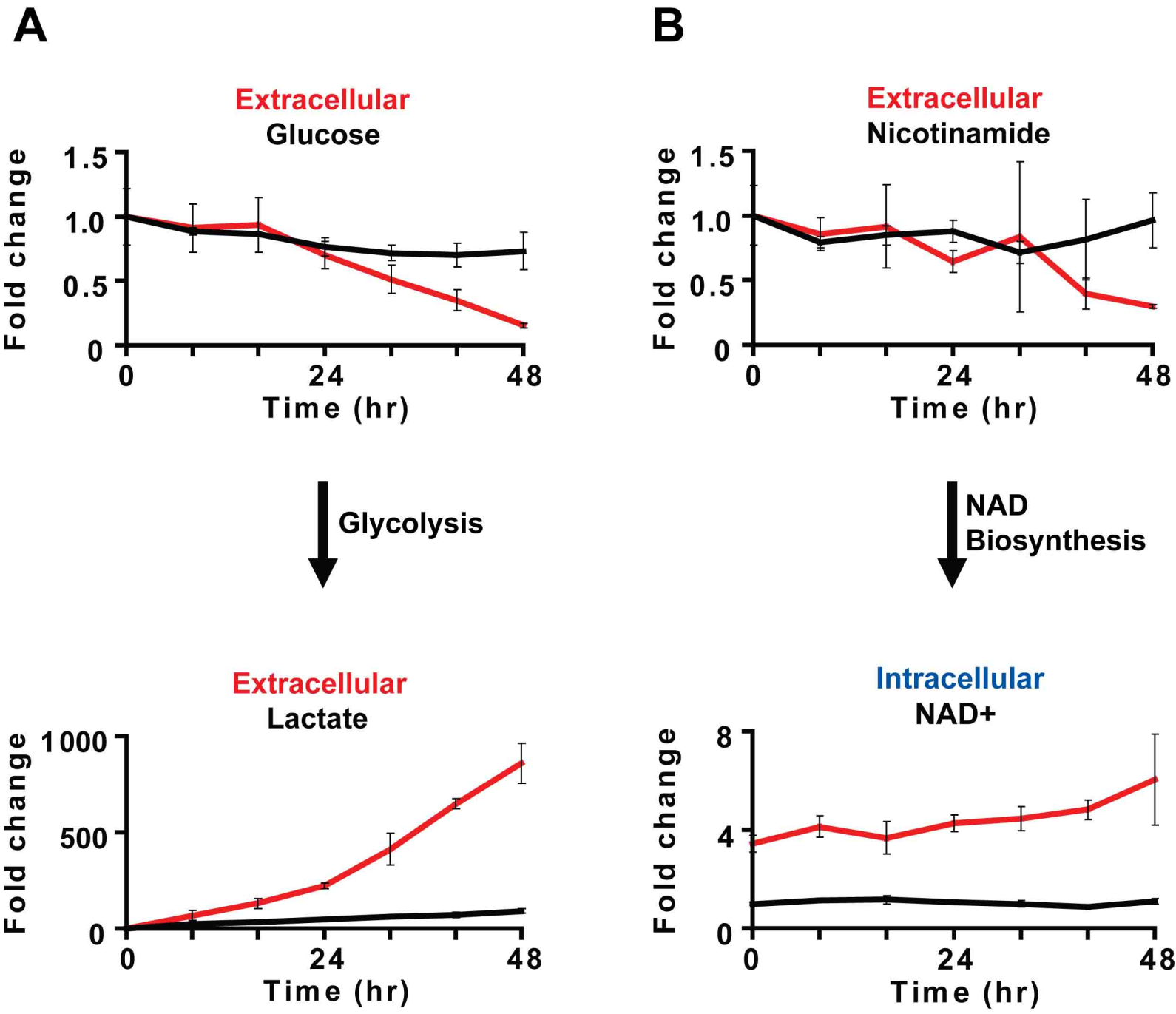

Figure S5. Conversion of Glucose into Lactate and Nicotinamide into NAD+ Are Increased by *Plasmodium* Infection

A

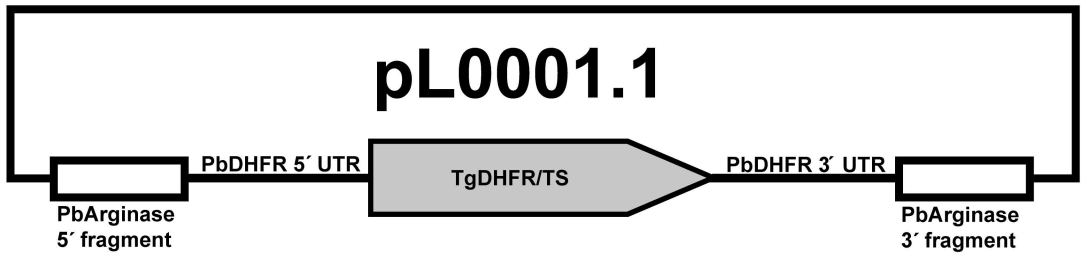

B

Wild-type locus fragment:

3513 bp

Knockout locus fragment:

6682 bp

C

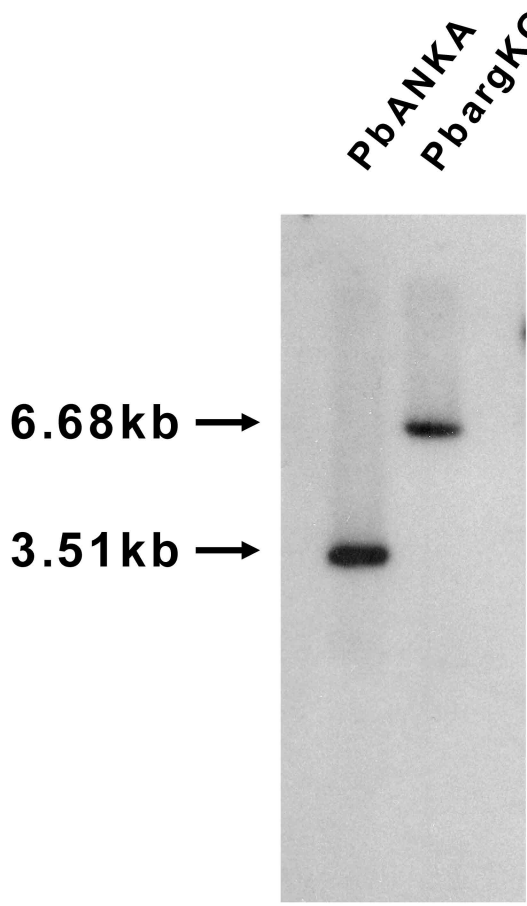

Figure S6. *P. berghei* Arginase Knockout

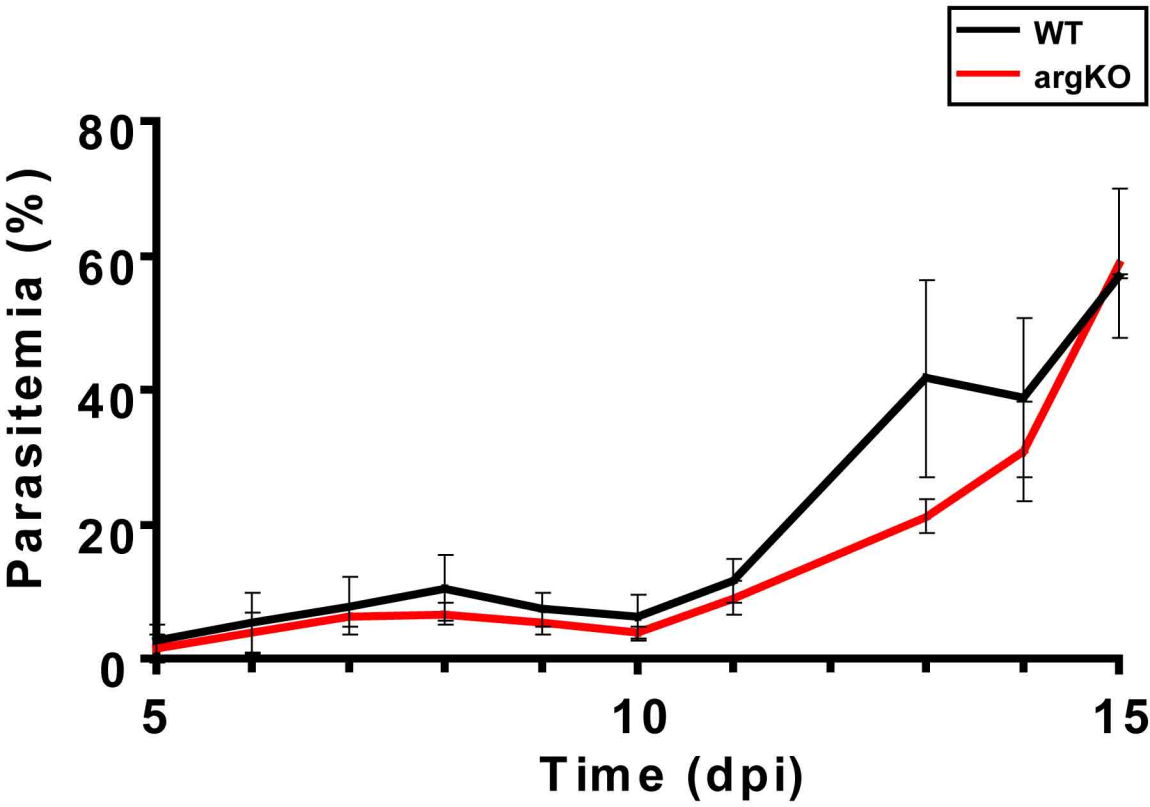

Figure S7. Parasitemia in WT and argKO *P. berghei* (ANKA) Infected BALB/c Mice

References

Bajad, S.U., Lu, W., Kimball, E.H., Yuan, J., Peterson, C., and Rabinowitz, J.D. (2006). Separation and quantitation of water soluble cellular metabolites by hydrophilic interaction chromatography-tandem mass spectrometry. J Chromatogr A *1125*, 76-88.

Bozdech, Z., Llinas, M., Pulliam, B.L., Wong, E.D., Zhu, J., and DeRisi, J.L. (2003). The transcriptome of the intraerythrocytic developmental cycle of Plasmodium falciparum. PLoS biology *1*, E5.

Ginsburg, H. (2006). Progress in in silico functional genomics: the malaria Metabolic Pathways database. Trends Parasitol *22*, 238-240.

Janse, C.J., Ramesar, J., and Waters, A.P. (2006). High-efficiency transfection and drug selection of genetically transformed blood stages of the rodent malaria parasite Plasmodium berghei. Nat Protoc *1*, 346-356.

Lambros, C., and Vanderberg, J.P. (1979). Synchronization of Plasmodium falciparum erythrocytic stages in culture. J Parasitol *65*, 418-420.

Lu, W., Kimball, E., and Rabinowitz, J.D. (2006). A high-performance liquid chromatography-tandem mass spectrometry method for quantitation of nitrogen-containing intracellular metabolites. J Am Soc Mass Spectrom *17*, 37-50.

Saldanha, A.J. (2004). Java Treeview--extensible visualization of microarray data. Bioinformatics *20*, 3246-3248.

Trager, W., and Jensen, J.B. (1976). Human malaria parasites in continuous culture. Science *193*, 673-675.